Mass and Charge Transport in a Cross-Linked Polyether-Based Electrolyte. The Role of Ion Pairs

Shahmahmood Obeidi[†] and Nicolaas A. Stolwijk*

Institute of Materials Physics and Sonderforschungsbereich 458, University of Münster, Wilhelm-Klemm-Strasse 10, D-48149 Münster, Germany

Steven J. Pas[‡]

Institute of Physical Chemistry, NRW International Graduate School of Chemistry, and Sonderforschungsbereich 458, University of Münster, Corrensstrasse 40, D-48149 Münster, Germany

Received September 9, 2005

ABSTRACT: In an amorphous solid polymer electrolyte the positive and negative ions are found to move much faster in the form of neutral pairs than individually. Although the fraction of ion pairs turns out to be small (less than 10%), the ion pairs provide the most significant contribution to the transport of cations being crucial for battery operation. This is a striking new result of a detailed comparison of tracer diffusion experiments and electrical conductivity measurements made on a cross-linked random copolymer of ethylene oxide and propylene oxide complexed with sodium iodide. The study utilizes radioactive isotopes of sodium and iodine in tiny amounts to trace the diffusivity of both ion species individually. The overall charge diffusivity due to the joint effect of cations and anions is monitored by impedance spectroscopy. A thorough evaluation of the experimental data shows that the diffusivity of all mobile species, although different in magnitude, shows the same temperature dependence. This is a consequence of ion transport in amorphous polymer electrolytes being coupled to the local motion of the polymer segments.

1. Introduction

Solid polymer electrolytes (SPEs) are ion-conducting, solvent-free materials usually composed of alkali-metal salts dissolved in a polyether matrix.[1,2] Over the past few decades, these systems have generated considerable interest, both technologically and scientifically, owing to their potential for use in lightweight rechargeable batteries. This potential as electrolyte material relies on the desirable combination of suitable mechanical properties (e.g., high flexibility but low fluidity, low mass density) and an appreciable conductivity, at least at elevated temperatures.

Widespread application of SPEs is restricted by the low ionic conductivities commonly observed at ambient temperatures.[3] Additionally, the fact that in most systems the anions are more mobile than the cations is disadvantageous for battery performance. It is believed that a basic understanding of the ionic transport mechanisms will provide us with clues to optimize the crucial properties of future SPE systems. In this context, it is advantageous to obtain a comprehensive characterization of each ion species in terms of its individual diffusivity as a function of temperature. This ion-specific data promises deeper insight than the overall dc conductivity which is usually measured as an average quantity for ionic mobility.

Recently, such detailed experimental information has been reported by our group for a complex based on poly(ethylene oxide) (PEO) and sodium iodide (NaI) with an O:Na ratio of 30.[4,5] For this $PEO_{30}NaI$ complex it was found that the radiotracer diffusivity of Na and I as well as the dc conductivity displayed different temperature dependences. Specifically, it was found that the sum of the cation and anion tracer diffusivity exceeded the charge diffusivity as deduced from the dc conductivity with the aid of the Nernst−Einstein equation. These observations could be rationalized within an empirical model which is based on the formation of mobile cation−anion pairs.[6] Such electrically neutral pairs contribute to cation and anion mass transport but evidently not to charge transport. However, the most surprising conclusion of this study was that the impact of pair formation on the diffusion of the slower ionic species (i.e., Na) is quite large. In fact, it was concluded that at all temperatures measured, Na transport was dominated by a small fraction (<0.1) of highly mobile pairs, presumably in a close-contact configuration.

As the conclusions of this earlier $PEO_{30}NaI$ study are rather unexpected, the question arises as to whether they may be generalized to other SPE systems. PEO-based electrolytes suffer from the partial crystallization of the polymer below the melting temperature (342 K) of pure poly(ethylene oxide). The heterogeneous semicrystalline state is characterized by a low conductivity which steeply decreases with decreasing temperature. For this reason, the previous diffusion and conductivity measurements on $PEO_{30}NaI$ were carried out over the temperature range from 340 to 453 K where the complex forms a highly viscous melt. To obtain electrolytes which are fully amorphous at room temperature, PEO may be copolymerized with an appropriate fraction of poly(propylene oxide) (PPO) which shows no crystallization at all. Additional cross-linking may lead then to an improvement of the mechanical stability.

The present paper explores the ionic transport properties of a complex consisting of NaI dissolved in cross-linked PolyG 83-48 (Arch Chemicals). PolyG is a trifunctional random copolymer of ethylene oxide (EO) and propylene oxide (PO) in a 4:1 mole ratio and is similar to the so-called 3PEG polymer host used in several

* Corresponding author. E-mail: stolwij@uni-muenster.de.
[†] E-mail: obeidish@nwz.uni-muenster.de.
[‡] E-mail: stpas@uni-muenster.de

10.1021/ma0519718 CCC: $30.25
Published on Web 11/15/2005

studies by the Monash group.[7−9] Specifically, for PolyG$_{20}$NaI with an O-to-Na ratio of 20, the tracer diffusion coefficients of ^{22}Na and ^{125}I are correlated with the ionic conductivity over a wide temperature range. It will be shown that the data are well described by the previously developed model based on neutral ion pairs. In particular we find that the Na tracer diffusivity is almost completely due to Na−I pair migration. By contrast, the tracer diffusivity of I nearly coincides with the effective diffusivity of single anions. Altogether, it will be shown that a small fraction of ion pairs with high mobility play a significant role in cation migration but influences the transport capacity of anions only to a minor extent.

2. Experiments

2.1. Synthesis and Characterization. The liquid polyether triol, traded as PolyG 83-48, a hydroxy-terminated random poly(oxyethylene-*co*-oxypropylene) of ca. 3600 g/mol molecular weight with an EO:PO ratio of 4:1, was generously donated by Arch Chemicals, Inc. The as-received polyol was purified by dissolving in milli-Q water, to remove polar impurities, and subsequently washed several times with hexane to remove organic impurities. The triol was extracted from water with dichloromethane, which was later removed by rotary evaporation, and then dried under vacuum at 380 K for 5 days. At the end of this procedure the polyol had a water content undetectable by Karl Fisher reagent. Furthermore, ^{13}C solid-state nuclear magnetic resonance showed no evidence of residual chlorinated solvent. The purified PolyG was then transferred to a high purity argon glovebox where all further operations took place. Electrolytes were prepared by dissolving an appropriate amount of anhydrous NaI salt (99.999%, Aldrich) into the liquid polyol at 340 K. Polyurethane elastomers were prepared by cross-linking the polyol/salt solution with a stoichiometric amount of hexamethylene diisocyanate over a minimal amount (<0.01 g) of Thorcat 535 catalyst (Thor Especialidades, S. A.). The resulting viscous liquid was poured into molds with the required cylindrical sample geometry (diameter 6 mm, height 8 mm), and after a 24 h cure period, a tough elastomeric polyurethane was obtained.

Phase behavior was determined by differential scanning calorimetry (DSC) at a scanning rate of 10 K/min using a Netzsch DSC 204. Temperature and heat flow were calibrated using cyclohexane over the range 173 to 313 K. Transitions are reported from their onset. Samples were accurately weighed and sealed in aluminum pans in an argon drybox. The sealed pan was placed in an oven at 333 K for 20 min and then quenched in liquid nitrogen before being transferred to a previously cooled DSC head. Upon heating cross-linked pure PolyG (without NaI) shows a glass transition at 210 K, crystallization at 234 K, and melting at 251 K. In contrast, PolyG$_{20}$NaI undergoes a glass transition at about 231 K, but no crystallization is observed. This means that the complex of interest appears as a single amorphous phase at all temperatures investigated (243−393 K).

The mass density of PolyG$_{20}$NaI was determined as 1.24 g/cm^3 at room temperature. To this end appropriate samples of the complex were weighted in air and in dodecane. Silicon with a known density of 2.33 g/cm^3 was used as a calibration standard.

2.2. Conductivity Measurements. Variable temperature ac impedance spectroscopy was carried out using a Novocontrol α-S high-resolution broadband dielectric analyzer with Quatro temperature management apparatus. Samples were cast into a locally designed stainless steel cylindrical cell (outer and inner electrode diameters of 89.5 and 54.6 mm, respectively) with a cell constant ca. 0.036 cm. The sealed cell was heated to 333 K for 20 min and then measured from 123 to 373 K. Conductivity samples were made from the same batch as the diffusion samples (see below).

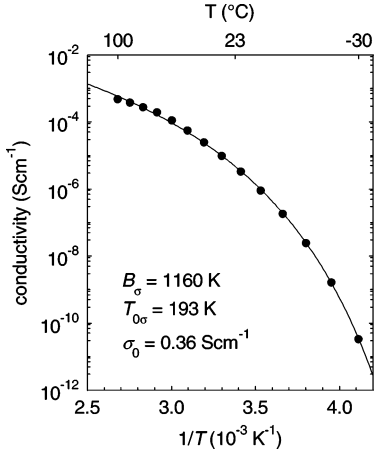

Figure 1. The dc conductivity of PolyG$_{20}$NaI as a function of inverse temperature resulting from ac impedance measurements. The solid line represents a fit of the VTF function characterized by the indicated parameter values.

Figure 1 shows the dc conductivity σ_{dc} as a function of inverse temperature from 243 to 373 K. For the sake of comparison with the literature, our results have been fitted by the Vogel−Tamann−Fulcher (VTF) equation $\sigma_{dc} = \sigma_0 \exp(-B_\sigma/(T - T_{\sigma_0}))$ yielding $B_\sigma = 1157$ K, $T_{\sigma_0} = 193$ K, and $\sigma_0 = 0.36\ \Omega^{-1}\text{cm}^{-1}$ (solid line). A more meaningful description is given later on in terms of the charge diffusivity D_σ within the ionic transport model presented below.

2.3. Radiotracer Diffusion Measurements. Radiotracer procedures were carried out under an inert atmosphere, using a nitrogen-flushed glovebox. Thin films of PEO$_{30}$NaI (typical thickness 40 μm) which had been doped with either ^{22}Na (half-life 2.6 a, γ energy 1.275 MeV) or ^{125}I (60 d, 30 keV) were used as source of radioactive ions. Details of the preparation procedure can be found elsewhere.[5] One or more pieces of radioactive film were pressed onto the sample within its cylindrical mold using a PTFE screw cap and an intermediate disk. Prior to this, the upper face of the sample had been flattened perpendicularly to the cylinder axis. After enclosing the PTFE mold in an aluminum container, diffusion annealing was carried out at temperatures between 296 and 393 K in a preheated oil-bath thermostat and stopped by quenching the Al container in water. In assessing the effective length of the diffusion anneal, corrections for heating-up and cooling-down were applied which never exceeded 3 min in total. These corrections were based on separate calibration runs using a similar annealing assembly which contained a thermocouple inside a dummy sample.

Serial sectioning was performed using a rotary microtome (Leica LM 2165) with a cold chamber (Leica LN21). Optimal operation was achieved for 20 μm sections and sample-cutting temperatures of about 225 K. Prior to sectioning, the (stack of) source film(s) was (were) removed from the sample. Because of this removal and the large penetration depths observed (1 mm or more; see below), the thickness of the diffusion source does not play a significant role. Then 50−100 sections were taken to determine the diffusion profile. Thicker sections were obtained by putting together two or more standard sections. Subsequently, the radioactivity of each section was counted with the aid of a well-type NaI scintillation crystal, correcting for background effects.

Typical diffusion profiles are shown in Figure 2 for ^{22}Na and in Figure 3 for ^{125}I. These profiles are fitted either by the complementary error function $c(x, t) = c_0\ \text{erfc}(x/2\sqrt{Dt})$ or by the Gaussian function $c(x, t) = c_0 \exp(-x^2/4Dt)$, where x denotes penetration depth, t diffusion time, D diffusion coefficient, and c concentration (in arbitrary radioactivity units). The prefactor c_0 is the concentration at $x = 0$. Both types of profile imply that the diffusivity D (obtained by fitting) is independent of x, providing evidence for the homogeneity of our samples.

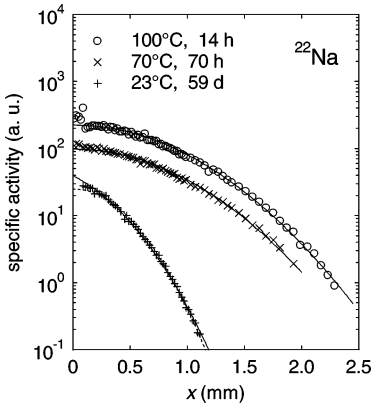

Figure 2. Diffusion profiles of ^{22}Na in PolyG$_{20}$NaI at various temperatures. Solid lines are fits of the Gaussian function. The shape of the 296 K profile is intermediate between Gaussian and erfc-type (dashed line).

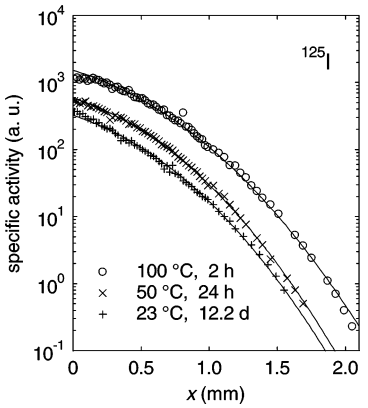

Figure 3. Diffusion profiles of ^{125}I in PolyG$_{20}$NaI at various temperatures. Solid lines are fits of the complementary error function.

A number of diffusion profiles were found to be intermediate between Gaussian- and erfc-types. An example is given by the 296 K profile in Figure 2. In such cases the diffusion coefficient was estimated by interpolating between the best-fit values arising from the two mathematical functions. The concomitant uncertainty in D is at most 15%.

The variation in profile shape points to differences in the boundary conditions during diffusion, which are likely to be related to the strength of the diffusion source. A sufficient amount of tracer atoms in the radioactive source film will be able to maintain a constant boundary concentration in the substate leading to an erfc-type depth distribution.[10] By contrast, prolonged annealing under weak-source conditions should lead to exhaustion of the radiotracer source. Accordingly, an initial erfc profile gradually changes over to a Gaussian profile.

The 296 K profiles in Figures 1 and 2 reveal that both ionic species diffuse considerably at room temperature. This means that microtome sectioning had to be done immediately following the oil-bath diffusion anneal. In all cases, it was ensured that the times needed for sectioning and other relevant procedures were short enough to warrant a reliable determination of the diffusion coefficient.

3. Diffusion Coefficients

Figure 4 displays the tracer diffusion coefficients D^*_{Na} and D^*_I that result from fitting of the ^{22}Na and ^{125}I penetration profiles, respectively. In this Arrhenius diagram, both sets of data reveal typical curvatures which are well described by a VTF function with the prefactor (D^*_{0Na}, D^*_{0I}), pseudoactivation energy (B^*_{Na}, B^*_I), and zero mobility temperature (T^*_{0Na}, T^*_{0I}) as adjustable parameters. The numerical results of VTF parameter fitting are listed in Table 1. At this stage of analysis, no deeper meaning should be attributed to these parameter values; they just allow for interpolation and comparison with literature data. In fact, the solid-line fits shown in Figure 4 result from a simultaneous fit of all data to be elucidated below.

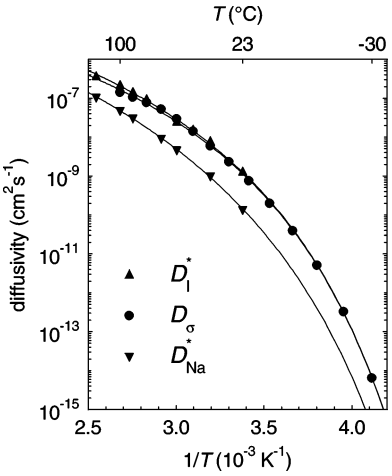

Figure 4. Tracer diffusion coefficients D^*_{Na} (down-triangles) and D^*_I (up-triangles) as a function of inverse temperature compared to the charge diffusivity D_σ (circles). The solid lines result from a simultaneous fit to all experimental data based on the ion transport model described in the text.

Table 1. VTF Parameters and Their Standard Deviation from Separate Fits to D^*_{Na}, D^*_I, and D_σ

Y	D^*_{0Y} (cm^2 s^{-1})	s_{DY} (%)	B^*_Y (K)	s_{BY} %	T^*_{0Y} (K)	s_{TY} %
Na	2.0×10^{-4}	225	1561	22	186	8.4
I	1.4×10^{-4}	138	1159	20	196	6.8
σ	1.55×10^{-4}	24	1240	3.3	191	0.7

It is seen that the anions migrate significantly faster than the cations, as commonly observed for SPE systems. In fact, the cation transport number t^*_+ given by

$$t^*_+ = \frac{D^*_{Na}}{D^*_{Na} + D^*_I} \tag{1}$$

varies from 0.10 at 296 K to 0.21 at 393 K. These minimum and maximum values associated with the end points of the temperature range investigated are smaller by roughly a factor of 2 than in a recent study of PEO$_{30}$NaI.[6] This indicates that the difference between the mobility of anions and cations is relatively large for PolyG$_{20}$NaI. The variation of t^*_+ with temperature is illustrated in Figure 5.

Figure 4 also shows the charge diffusivity which was calculated from σ_{dc} by using the Nernst−Einstein equation

$$D_\sigma \equiv \frac{\sigma_{dc} k_B T}{C_s e^2} \tag{2}$$

where k_B denotes Boltzmann's constant, T temperature, C_s salt concentration (i.e., number density), and e elementary charge. Again, the D_σ data can be reproduced by a separate VTF function (not shown in Figure 4) with the parameters $D^*_{0\sigma} = 1.55 \times 10^{-4}$ cm^2 s^{-1}, $B^*_\sigma = 1240$ K, $T^*_{0\sigma} = 191$ K also given in Table 1. The last two

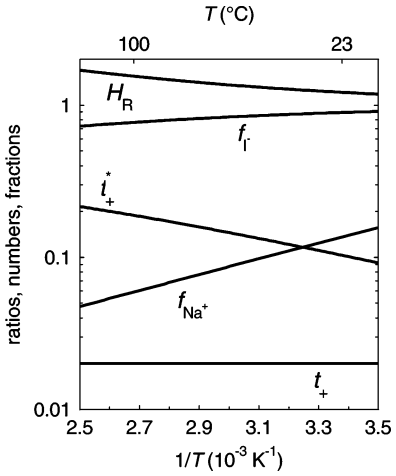

Figure 5. Temperature dependence of the Haven ratio H_R, the transport number t_+^*, the transference number t_+, and the fractional diffusivity components f_{Na^+} and f_{I^-}.

of these parameter values differ slightly from the corresponding values for σ_{dc} ($B_\sigma = 1157$ K, $T_{\sigma_0} = 193$ K) which is due to the fact that the charge diffusion coefficient contains an additional proportionality factor T, cf. eq 2.

By taking C_s in the denominator of eq 2 (instead of $2C_s$ being the number density of ions), then D_σ stands for the charge diffusivity per salt molecule; that is, D_σ comprises the joint effect of one cation and one anion. Therefore, D_σ may be compared with the sum of the tracer diffusion coefficients $D_{Na}^* + D_I^*$. Since it is seen in Figure 4 that D_I^* tends to be (slightly) larger than D_σ, the relationship $D_{Na}^* + D_I^* > D_\sigma$ certainly holds. This may be expressed in terms of the so-called Haven ratio H_R given by[11,12]

$$H_R = \frac{D_{Na}^* + D_I^*}{D_\sigma} \tag{3}$$

Indeed, Figure 5 shows that $H_R > 1$ holds for all temperatures investigated, ranging from 1.7 at 400 K to 1.2 at room temperature. This finding can be rationalized by assuming the occurrence of mobile cation−anion pairs. Evidently such electrically neutral $(NaI)^0$ pairs will contribute to mass transport (D_{Na}^*, D_I^*) but not to charge transport (D_σ). Therefore, the application of an ionic transport model, in which the thermal equilibrium between charged ions and neutral pairs plays a central role, is necessary.

4. Ionic Transport Model

Here we summarize the main features of a theoretical framework which was initially developed for the evaluation of diffusion and conductivity data on $PEO_{30}NaI$.[4,5] A full account of the model has been given elsewhere.[6]

Association of the single ions Na^+ and I^- and their subsequent dissociation may be represented by the reaction

$$Na^+ + I^- \rightleftharpoons (NaI)^0 \tag{4}$$

A basic assumption of the model is that larger aggregates do not play a significant role. Using the index p for $(NaI)^0$ pairs the corresponding concentrations (number densities) are designated as C_{Na^+}, C_{I^-}, and C_p which are subject to the constraints of charge neutrality, $C_{Na^+} = C_{I^-}$, and mass conservation, $C_{Na^+} + C_p = C_{I^-} + C_p = C_s$. Application of the mass action law to eq 4 leads to

$$r_p = k_p(1 - r_p)^2 \tag{5}$$

where $r_p \equiv C_p/C_s$ denotes the fraction of ion pairs with respect to the salt concentration. The (reduced) reaction constant k_p can be written as

$$k_p = k_{p0} \exp(-\Delta H_p/k_B T) \tag{6}$$

where ΔH_p represents the pair formation enthalpy while the dimensionless prefactor k_{p0} contains a corresponding entropy factor and the proportionality factor C_s. Solving eq 5 yields r_p as a function of temperature, i.e.,

$$r_p = 1 + (1 - \sqrt{1 + 4k_p})/2k_p \tag{7}$$

For small values of the pair fraction the expansion $r_p \approx k_p - 2k_p^2$ may provide a useful approximation.

Each ionic species X = Na^+, I^-, or p = $(NaI)^0$ is characterized by its "true" diffusivity D_X. A preliminary analysis like the one reported for $PEO_{30}NaI$[6] indicated that these ionic diffusivities may be very similar concerning their (VTF-type) temperature dependence but dissimilar in magnitude. This circumstance is also strongly suggested by the almost parallel data curves in Figure 4. Therefore, we adopt the general expression

$$D_X = D_X^0 \exp(-B/(T - T_0)) \tag{8}$$

with the initially unknown VTF parameters (B, T_0) and prefactors ($D_{Na^+}^0$, $D_{I^-}^0$, D_p^0). The underlying idea is that all transport processes in SPE systems are driven by the segmental motion of the polymer chains as corroborated by previous work.[13,15,16]

Considering the overall migration of, e.g., Na, we have to distinguish between a contribution of the single ions Na^+ and a contribution due to the $(NaI)^0$ pairs. A more elaborate treatment[6] shows that this can be formulated in terms of "effective" diffusivities $\hat{D}_X$ defined as

$$\hat{D}_X = \frac{C_X D_X}{C_s} \tag{9}$$

In this expression the true diffusivity D_X is multiplied by the probability C_X/C_s that the configuration X = Na^+, I^-, or p = $(NaI)^0$ occurs. Eventually, the three different sets of experimental data can be described by the equations

$$D_{Na}^* = \hat{D}_{Na^+} + \hat{D}_p \tag{10}$$

$$D_I^* = \hat{D}_{I^-} + \hat{D}_p \tag{11}$$

$$D_\sigma = \hat{D}_{Na^+} + \hat{D}_{I^-} \tag{12}$$

with

$$\hat{D}_{Na^+} = (1 - r_p)\, D_{Na^+}^0 \exp(-B/(T - T_0)) \tag{13}$$

$$\hat{D}_{I^-} = (1 - r_p)\, D_{I^-}^0 \exp(-B/(T - T_0)) \tag{14}$$

$$\hat{D}_p = r_p\, D_p^0 \exp(-B/(T - T_0)) \tag{15}$$

Here $C_{Na^+}/C_s = C_{I^-}/C_s = 1 - r_p$ was used.

Table 2. Model Parameters and Their Statistical Error from a Simultaneous Fit to D^*_{Na}, D^*_I, and D_σ

B (K)	T_0 (K)	$D^0_{Na^+}$ ($cm^2\ s^{-1}$)	$D^0_{I^-}$ ($cm^2\ s^{-1}$)	D^0_p ($cm^2\ s^{-1}$)	k_{p0}	ΔH_p (eV)
1238	191	3.0×10^{-6}	1.6×10^{-4}	5.0×10^{-4}	4.3	0.12
5%	1%	200%	25%	30%	20%	8%

5. Data Evaluation

The three sets of experimental data displayed in Figure 4 were simultaneously fitted by eqs 10−12 with their specific formulation outlined above. The fits are shown in Figure 4 as continuous curves which closely reproduce the data points. The corresponding best estimates of the free parameters B, T_0, $D^0_{Na^+}$, $D^0_{I^-}$, D^0_p, k_{p0}, and ΔH_p are compiled in Table 2 together with their statistical uncertainty. Although the number of free parameters, i.e., seven, may seem large, it favorably relates to the available experimental information. Indeed, our initial "ad hoc" approach, in which each individual set of data was separately fitted by the VTF function, even required nine adjustable parameters (Table 1), however, without yielding significantly better adjustments. The validity of the model is further sustained by the generally modest uncertainty in the parameter values (Table 2). The impact of these parameter values values will be discussed now in detail.

ΔH_p and k_{p0} are found to be 0.12 (±8%) eV and 4.3 (±20%), respectively. We note that ΔH_p and k_{p0} values of similar magnitude have been found in other polymer electrolytes.[4,17] The positive value of ΔH_p may be surprising at first glance but can be understood from the strong binding of single cations to the ether oxygens of the polymer. This relates to the fact that the salt, with a relatively high lattice energy, dissolves in the polymer at all. The positive ΔH_p value leads to an increase of the number of ion pairs with increasing temperature, which is graphically displayed in Figure 6. To be specific, r_p rises from ∼0.01 at 240 K to ∼0.1 at 400 K.

Pair formation may be viewed as the initial stage of salt precipitation observed in SPE systems at high temperatures.[18,19]

The best estimate of the prefactor $k_{p0} = 4.3$ corresponds to a change in entropy upon pair formation, i.e., $\Delta S_p \approx 1.5 k_B$. The positive value of ΔS_p relates to the gain in configurational freedom of the polymer segments upon release of the oxygen-coordinated Na^+ ions acting as network cross-links.[20] For this reason, pair formation in polymer electrolytes has been characterized in the literature as "entropy driven".[17,20]

The temperature dependence of the true diffusivities is characterized by the VTF parameter values $B = 1238$ (±5%) K and $T_0 = 191$ (±1%) K. These values do not differ significantly from the corresponding separate values for D_σ given in Table 1. The reason for some difference lies in the fact that simultaneous fitting within the ionic transport model also includes the tracer diffusivities. The relatively small magnitude of this difference, however, relates to the fact that (the temperature dependence of) D_σ is only slightly affected by pair formation as $1 - r_p \approx 1$ (cf. eqs 12−14). However, the wide temperature interval of the D_σ data and the small scatter in all experimental data lead to a considerable reduction of the statistical uncertainties.

The present T_0 value lies 40 K below the glass transition temperature of the complex (231 K) given in section 2. This agrees well with established empirical rules for these parameters.[21] Also the resulting B value falls into the common range for polymer electrolytes.[2,22]

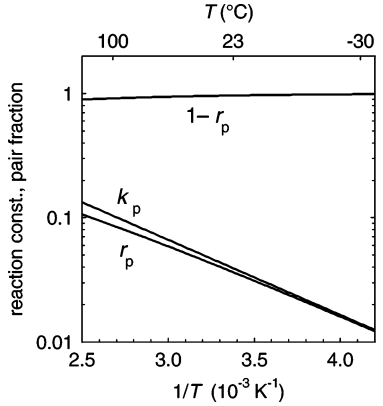

Figure 6. Temperature dependence of the ion-pairing reaction rate k_p and the $(NaI)^0$ pair fraction r_p as resulting from the model described in the text. The fraction of either single ion species, $1 - r_p$, is also displayed.

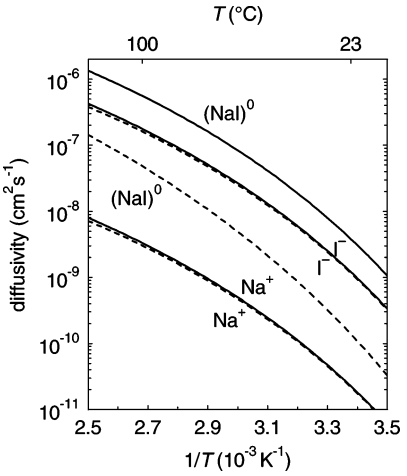

Figure 7. True diffusivity (solid lines) of single ions (D_{Na^+},D_{I^-}) and ion pairs (D_p) revealing the same VTF temperature dependence characterized by $B = 1238$ K and $T_0 = 191$ K. The corresponding effective diffusivity (dashed lines) is distinctly smaller for $(NaI)^0$ pairs ($\hat{D}_p = r_p D_p$) but almost coincides with the true diffusivity for Na^+ and I^- ($\hat{D}_{Na^+} = (1 - r_p)D_{Na^+}$, $\hat{D}_{I^-} = (1 - r_p)D_{I^-}$).

Figure 7 compares the true diffusivities D_X of the three ionic species with their effective counterparts $\hat{D}_X$ (cf. eq 9). It is seen that D_{Na^+}, D_{I^-}, and D_p (solid lines) run parallel as dictated by eq 8. The differences in magnitude are due to differences in the prefactors D^0_X. Single cations are the slowest species as exemplified by the comparatively small prefactor $D^0_{Na^+} = 3.0 \times 10^{-6}$ (± 200%) $cm^2\ s^{-1}$. This finding is a direct result of the strong bonds formed between the cations and the polymer matrix. The large statistical error[23] in $D^0_{Na^+}$ relates to the fact that the contribution of Na^+ both to D^*_{Na} and D_σ is almost insignificant (see below). In general, the uncertainty in preexponential factors tends to be larger than in the other parameters since they involve the wide extrapolation toward $1/T = 0$ (cf. Table 1).

Single anions characterized by $D^0_{I^-} = 1.6 \times 10^{-4}$ (± 25%) $cm^2\ s^{-1}$ are faster than the cations by a factor of 53. This reflects the higher degree of freedom of the anions which only indirectly interact with the polymer chains, i.e., through Coulombic forces with the cations. The most mobile species, however, are the ion pairs with

$D_p^0 = 5.0 \times 10^{-4}$ ($\pm$ 30%) cm^2 s^{-1}. Consequently, the ion pairs have a true diffusivity three times that of the anions and 167 times the cations. Such a high pair diffusivity can hardly be reconciled with solvent-shared or solvent-separated pairs[24] which are bound to the polymer chains via oxygen coordination of the cation member. The present result should be rather interpreted in terms of freely moving contact pairs. This view is corroborated by the finding that the actual values of the (true) pair diffusivity amount to as high as 1.0×10^{-6} cm^2 s^{-1} (see Figure 7). Such values are typical for small neutral molecules in polymer melts.[25]

The effective diffusivities are displayed in Figure 7 as dashed lines. For Na^+ and I^- it is hard to distinguish the effective diffusion coefficients from the true ones. This is due to the fact that $C_{Na^+}/C_s = C_{I^-}/C_s \approx 1 - r_p$ is close to one since $r_p \ll 1$. In contrast, $\hat{D}_p = r_p D_p$ is much smaller than D_p for similar reasons. Moreover, the $\hat{D}_p$ curve in Figure 6 differs in slope from the other curves. Its greater steepness stems from the pair formation energy ΔH_p which enters r_p via k_p.

6. Discussion

For a critical discussion of the present results we compare the different effective diffusivities among each other and with the experimentally determined diffusion coefficients. For this purpose transport/transference numbers and fractional diffusivity components (to be introduced below) are useful quantities.

In contrast to the transport number given in eq 1, the transference number t_+ is based on the effective diffusivities of charged species only, viz.,

$$t_+ = \frac{\hat{D}_{Na^+}}{\hat{D}_{Na^+} + \hat{D}_{I^-}} = \frac{D_{Na^+}}{D_{Na^+} + D_{I^-}} = \frac{D^0_{Na^+}}{D^0_{Na^+} + D^0_{I^-}} \qquad (16)$$

Thus, it accounts for the relative contribution of Na^+ to the charge diffusivity D_σ (cf. eq 12). It should be noted that according to eq 16 t_+ is a temperature-independent constant determined by $D^0_{Na^+}$ and $D^0_{I^-}$. For PolyG$_{20}$NaI we obtain $t_+ = 0.02$ (see Figure 5) which is an extremely small number. On the other hand, the T dependence of t_+^* (Figure 5) can now be understood from the varying contribution of $\hat{D}_p$ to D^*_{Na} and D^*_I as a function of temperature; see eqs 1, 10, and 11.

In Figure 8, the experimentally determined diffusion coefficients (symbols) are compared with the effective diffusivities arising from model fitting (dashed lines). In the temperature range presented, $\hat{D}_{Na^+}$ is about an order of magnitude smaller than $\hat{D}_p$ and $\hat{D}_p$ is lower than $\hat{D}_{I^-}$ by roughly a factor of 5. This has several consequences.

First, the iodine tracer diffusivity D^*_I is only slightly larger than $\hat{D}_{I^-}$, that is

$$D^*_I \approx \hat{D}_{I^-} \qquad (17)$$

This means that iodine transport predominantly takes place in the single-ion configuration. Using eq 11 this can be formulated in terms of the fractional I^- component f_{I^-} defined as

$$f_{I^-} \equiv \frac{\hat{D}_{I^-}}{D^*_I} = \frac{\hat{D}_{I^-}}{\hat{D}_{I^-} + \hat{D}_p} = \left(1 + \frac{r_p D^0_p}{(1 - r_p) D^0_{I^-}}\right)^{-1} \qquad (18)$$

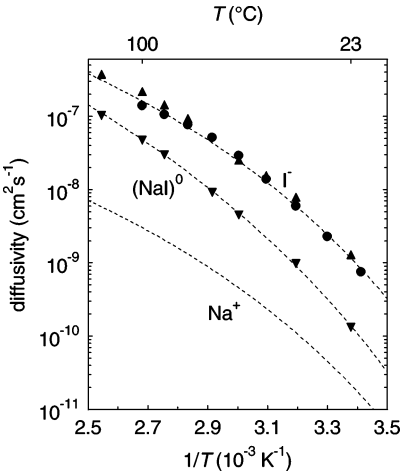

Figure 8. Comparison of the experimentally determined diffusion coefficients D^*_{Na} (down-triangles), D^*_I (up-triangles), and D_σ (circles) with the effective diffusivities $\hat{D}_X$ (dashed lines) for $X = Na^+$, I^-, and $p = (NaI)^0$.

Figure 5 shows that f_{I^-} moderately changes from 89% at room temperature to 74% at the high end of the temperature range investigated (400 K). Thus, ion pairs only provide a minor contribution to D^*_I.

Second, D_σ virtually coincides with $\hat{D}_{I^-}$, i.e.,

$$D_\sigma \approx \hat{D}_{I^-} \qquad (19)$$

As a consequence, charge transport is almost exclusively due to the anions. Cations only carry 2% of the electrical current, as already indicated above in terms of the temperature-independent transference number t_+. Obviously, this circumstance is disfavorable for battery operation.

Third, the D^*_{Na} data are reproduced by the $\hat{D}_p$ curve to a very good approximation, viz.,

$$D^*_{Na} \approx \hat{D}_p \qquad (20)$$

Thus, Na transport is dominated by the $(NaI)^0$ pairs. Accordingly, the fractional single-ion component

$$f_{Na^+} \equiv \frac{\hat{D}_{Na^+}}{D^*_{Na}} = \frac{\hat{D}_{Na^+}}{\hat{D}_{Na^+} + \hat{D}_p} = \left(1 + \frac{r_p D^0_p}{(1 - r_p) D^0_{Na^+}}\right)^{-1} \qquad (21)$$

is small. It varies from about 14% at room temperature to 5% at 400 K, as illustrated by Figure 5. The approximate equality of eq 20 as well as those of eqs 17 and 19 are visualized in Figure 8 by the near coincidence of the dashed lines ($\hat{D}_X$) with the experimental data.

The present findings may be compared with previous results obtained from PEO$_{30}$NaI.[4,6] For that complex a similar picture was observed, that is, a predominance of single anions in both iodine and charge transport along with a predominance of ion pairs in sodium transport. However, for PolyG$_{20}$NaI the situation is more extreme as reflected by a transference number and fractional diffusivity components closer to either 0 or 1. In both systems we observe pair fractions r_p of similar magnitude over the respective temperature ranges. Apparently, the moderate differences in ΔH_p (0.19 for PEO$_{30}$NaI) and k_{p0} (14 for PEO$_{30}$NaI) reflect to a large extent the dissimilar glass transition and/or melting temperatures of the complexes. Furthermore, PEO$_{30}$NaI and PolyG$_{20}$NaI reveal the same order in the magnitude

of the individual true diffusivities, i.e., $D_p > D_{I^-} > D_{Na^+}$. It is remarkable, however, that the single anions are relatively fast in PolyG_{20}NaI. This may be recognized from $D^0_{I^-}/D^0_{Na^+} = 53$ (cf. Table 2) compared to 8 for PEO_{30}NaI.[5]

In discussing possible causes for the difference in the relative single-anion mobility one naturally has to consider the dissimilarities between the complexes. With respect to PEO_{30}NaI, ionic migration in PolyG_{20}NaI may be additionally affected by the random copolymerization with propylene oxide, the cross-linking through hexamethylene diisocyanate, and the increased ionic density (note that the smaller O-to-Na ratio, i.e., 20, designates the higher salt concentration). Not only the copolymerization and the cross-linking but also the increased ionic density will change the mechanical properties. In the latter case, this is due to the intra- and interchain coordination of the cations by the ether oxygen atoms leading to reductions in configurational freedom of the polymer matrix. We suppose, however, that the changes in the mechanical properties are reflected by shifts in the values of the VTF parameters B (521 K for PEO_{30}NaI[4]) and T_0 (225 K for PEO_{30}NaI[4]). Nevertheless, a direct effect of C_s on ionic transport may additionally occur.

Molecular dynamics calculations[14,15] provide evidence that low salt concentrations lead to the formation of ionic clusters (also termed salt-rich domains). Concomitantly, the regions between the clusters possess relatively low ionic densities. In contrast, for higher salt concentrations a more homogeneous morphology of the polymer electrolyte is observed in the computer simulations.[14,15] We speculate that anion migration across the regions of low ionic density may be hampered due to the constraint of local charge neutrality within Debye length scales. This argument holds for the faster of the two ionic species, that is, the anion. Conversely, for the slow cation, the mobility may be enhanced in low-density regions owing to reduced site blocking. These two opposite effects predict a lower value for the ratio $D^0_{I^-}/D^0_{Na^+}$ in the case of PEO_{30}NaI than for PolyG_{20}NaI, in agreement with our experiment-based results.

Conclusions

Ion transport properties in the cross-linked EO/PO-based polymer electrolyte PolyG_{20}NaI have been characterized by means of conductivity and radiotracer diffusion measurements. The experimental results can be explained within an empirical model which is based on the occurrence of single cations, single anions, and their pairs as mobile species. A quantitative evaluation of the model parameters leads to the following conclusions: (i) Neutral cation−anion pairs contribute significantly to mass transport but not to charge transport. (ii) The diffusivities of ion pairs and single ions obey the same VTF temperature dependence. (iii) Cation transport almost exclusively takes place in the highly mobile ion-pair configuration. (iv) The true cation transference number is as low as 0.02 and independent of temperature. (v) The fraction of ion pairs increases with increasing temperature according to a pair formation enthalpy of about 0.1 eV.

Altogether, ion migration in PolyG_{20}NaI appears to be close to the degenerated case in which single cations are virtually immobile and single anions exclusively responsible for charge transport.

Acknowledgment. The authors thank H. Mehrer, A. Imre, W. Pröbsting, and S. Voss for helpful cooperation.

References and Notes

(1) Sadoway, D. R.; Mayes, A. M. *MRS Bull.* **2002**, *27*, 590.
(2) Gray, F. M. *Solid Polymer Electrolytes*; VCH: New York, 1991.
(3) Wright, P. V. *MRS Bull.* **2002**, *27*, 597.
(4) Stolwijk, N. A.; Obeidi, Sh. *Phys. Rev. Lett.* **2004**, *93*, 125901.
(5) Obeidi, Sh.; Zazoum, B.; Stolwijk, N. A. *Solid State Ionics* **2004**, *173*, 77.
(6) Stolwijk, N. A.; Obeidi, Sh. *Diffus. Defect Forum* **2005**, *237*, 1004.
(7) Bishop, A. G.; MacFarlane, D. R.; McNaughton, D.; Forsyth, M. *J. Phys. Chem.* **1996**, *100*, 2237.
(8) Bishop, A. G.; MacFarlane, D. R.; McNaughton, D.; Forsyth, M. *Solid State Ionics* **1996**, *85*, 129.
(9) Bishop, A. G.; MacFarlane, D. R.; Forsyth, M. *Electrochim. Acta* **1998**, *43*, 1453.
(10) Crank, J. *The Mathematics of Diffusion*; Clarendon Press: Oxford, U.K., 1995.
(11) Murch G. E.; Dyre J. C. *CRC Crit. Rev. Solid State Mater. Sci.* **1989**, *15*, 345.
(12) Voss, S.; Imre, A. W.; Mehrer, H. *Phys. Chem. Chem. Phys.* **2004**, *6*, 3669.
(13) Fontanella, J. J.; Wintersgill, M. C.; Smith, M. K.; Semancik, J.; Andeen, C. G. *J. Appl. Phys.* **1986**, *60*, 2665.
(14) Borodin, O.; Smith, G. D. *Macromolecules* **1998**, *31*, 8396.
(15) Borodin, O.; Smith, G. D. *Macromolecules* **2000**, *33*, 2273.
(16) Dürr, O.; Dieterich, W.; Nitzan, A. J. *Chem. Phys.* **2004**, *121*, 12732.
(17) Schantz, S. *J. Chem. Phys.* **1991**, *94*, 6296.
(18) Chiang, C. K.; Davis, G. T.; Harding, C. A.; Aarons, J. *Solid State Ionics* **1983**, *9−10*, 1121.
(19) Forsyth, M.; Payne, V. A.; Ratner, M. A.; de Leeuw, S. W.; Shriver, D. F. *Solid State Ionics* **1992**, *53−56*, 1011.
(20) Ratner, M. A.; Nitzan, A. *Faraday Discuss. Chem. Soc.* **1989**, *88*, 19.
(21) Ratner, M. A. *Polymer Electrolyte Reviews-1*; MacCallum, J. R., Vincent, C. A., Eds.; Elsevier: London and New York, 1987; Chapter 7.
(22) Bamford, D.; Reiche, A.; Dlubek, G.; Alloin, F.; Sanchez, J.-Y.; Alam, M. A. *J. Chem. Phys.* **2003**, *118*, 9420.
(23) Diffusivity prefactors D_0 enter the fitting procedure in the form of exp(ln D_0). The resulting standard deviations s_D in ln D_0 (absolute values) lead to uncertainty factors of exp($\pm s_D$). The specification $D_0 \pm 200\%$ corresponds to uncertainty factors 3 (high bound) and 1/3 (low bound).
(24) Bruce, P. G., Ed. *Solid-State Electrochemistry*; Cambridge University Press: Cambridge, U.K., 1997.
(25) Gee, R. H.; Boyd, R. H. *Polymer* **1995**, *36*, 1435.

MA0519718